Materials Chemistry and Physics xxx (2016) 1–9

Contents lists available at ScienceDirect

Materials Chemistry and Physics

journal homepage: www.elsevier.com/locate/matchemphys

The investigation of the production method influence on the structure and properties of the ferroelectric nonwoven materials based on vinylidene fluoride – tetrafluoroethylene copolymer

E.N. Bolbasov [a], K.S. Stankevich [a], E.A. Sudarev [a], V.M. Bouznik [b], V.L. Kudryavtseva [a], L.V. Antonova [c], V.G. Matveeva [c], Y.G. Anissimov [d, e], S.I. Tverdokhlebov [a, *]

[a] Tomsk Polytechnic University, 30 Lenin Avenue, Tomsk, 634050, Russian Federation
[b] All Russian Scientific Research Institute of Aviation Materials, 17 Radio str., Moscow, 105005, Russian Federation
[c] Federal State Budgetary Institution Research Institute for Complex Issues of Cardiovascular Disease, 6 Sosnovy Blvd, Kemerovo, 650002, Russian Federation
[d] Griffith University, School of Natural Sciences, Nathan, Queensland, Australia
[e] Queensland Micro- and Nanotechnology Centre, Griffith University, Nathan, Queensland, Australia

HIGHLIGHTS

- Production method affects properties of nonwoven polymer ferroelectric materials.
- Materials produced by electrospinning have more pronounced piezoelectric properties.
- Materials produced by electrospinning have higher strength and elongation.
- Cell adhesion is higher to the nonwoven materials produced by solution blow spinning.

GRAPHICAL ABSTRACT

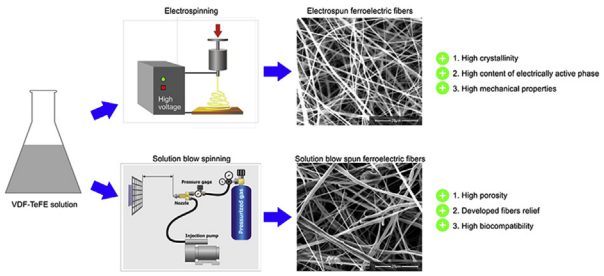

ARTICLE INFO

Article history:
Received 13 April 2016
Received in revised form
2 July 2016
Accepted 17 July 2016
Available online xxx

Keywords:
Ferroelectric polymer
Nonwoven materials
Vinylidene fluoride – tetrafluoroethylene copolymer (VDF-TeFE)
Electrospinning
Solution blow spinning

ABSTRACT

In the present work the production method influence (solution blow spinning and electrospinning) on the structure and properties of the ferroelectric nonwoven materials based on VDF-TeFE copolymer is investigated. It was shown that the nonwoven materials obtained by electrospinning have smooth cylindrical-shaped fibers with a narrow diameter distribution, whereas the nonwoven materials produced by solution blow spinning are characterized by multi-level spatial organization with the fibers having their own advanced morphology. By using DSC and XRD analysis it was found that the nonwoven materials obtained by electrospinning have higher content of the electrically active phases. Also these materials have higher strength owing to their morphological and structural features. It was shown that both types of nonwoven materials are non-toxic. A higher adhesion of stem cells and cells from EA-hy 926 cell line to nonwoven materials produced by solution blow spinning was observed.

1. Introduction

Polyvinylidene fluoride (PVDF) and its copolymers with trifluoroethylene (VDF-TrFE) and tetrafluoroethylene (VDF-TeFE) are

* Corresponding author.
E-mail address: tverd@tpu.ru (S.I. Tverdokhlebov).

http://dx.doi.org/10.1016/j.matchemphys.2016.07.041
0254-0584/

known to have a number of beneficial properties such as high chemical resistance, an ability to dissolve in organic solvents, an ability to form fibers, high hydrophobicity, thermoplasticity, and good mechanical properties [1]. All these features make it possible to create a wide range of PVDF and its copolymers-based nonwoven materials for various applications [2]. Such materials are used for membrane distillation [3,4], secondary battery separators [5,6], and polymer electrolytes production [7].

PVDF and its copolymers belong to a group of the most electroactive polymers because of their significant dipole moment directed perpendicular to the axis of the polymer chain. It arises due to the high electronegativity of fluorine atoms present in PVDF. The significant dipole moment allows PVDF and its copolymers to form crystalline structures with piezoelectric and ferroelectric properties at a particular conformation of the polymer macromolecules. There are three main crystalline phases α, β, and γ. The α − form is characterized by a monoclinic lattice in which the chain conformation (*TGTG-*) has opposite dipole moments, so in general it is non-polar. The β − crystalline form has an orthorhombic lattice with polar cell units in which chains have planar zigzag conformation. The γ − form is comprised of polar cell units with the chain conformation $T_3GT_3G^-$. Among these crystalline forms, *β* is the most electrically active, as it has the most significant dipole moment ($\approx 8 \times 10^{-30}$ cm) [8].

Piezoelectric and ferroelectric properties of PVDF and its copolymers are attractive for the creation of “smart” materials - devices capable of changing their characteristics (size, surface charge density, conductivity, dielectric constant, etc.) in response to the external mechanical or electrical forces. Smart nonwoven materials made of PVDF and its copolymers are used for western blot [9], for energy generators [10], sensors [11], and microrobots production [12]. One of the prospective application fields is the use of PVDF and its copolymers for the development of smart implants and scaffolds for the tissue engineering. Such devices could affect cells and tissues by means of an electrical power without implanting electrodes and the use of external voltage source owing to their piezoelectric and ferroelectric properties [24,25]. It is supposed that PVDF and its copolymers could be applied for cardiovascular tissue engineering [13] [14], spinal cord injury, nerve [15,16], esophagus [17], and bone tissue regeneration [18–20], wound healing [21], drug release [22], and cell biology [23].

One of the most widespread methods of PVDF and its copolymers-based nonwoven material fabrication is electrospinning (ES) [26,27]. Nonwoven materials produced by ES have a narrow fiber diameter distribution, good mechanical strength, and high biocompatibility [28]. However, the use of ES for implants and scaffold production is limited due to the following reasons: complexity of obtaining nonwoven materials with a thickness greater than 500 μm; insufficient pore size prevents infiltration of cells and tissues in a bulk of the nonwoven materials; selectivity to the relative dielectric constant of the solvent used to make a spinning solution [29].

An alternative method of producing the nonwoven materials from polymer solutions is a solution blow spinning (SBS) or Air Spinning (AS) which uses the high-pressure gas stream to form a nonwoven. In comparison with ES this method has a high efficiency, low cost of the technological equipment, allows the use of multiple molding nozzles, and the formation of nonwoven materials *in situ* [30–32].

The technological parameters and their influence on the properties of nonwoven materials obtained by SBS from various polymers and the scope of their potential applications are being actively studied [33,34]. A comparative analysis of the nonwoven materials produced by SBS and ES from a variety of biodegradable polymers for tissue engineering applications had been carried out [35–38].

It is known that the processing conditions largely determine the crystalline structure and, thus, a set of the physicochemical properties of PVDF and its copolymers [39]. Today the effect of the technological parameters on the structure and properties of the PVDF and its copolymers-based nonwoven materials produced by electrospinning is well studied [40–42]. However, a lack of comparative studies of the structure and properties of ferroelectric nonwoven materials obtained by SBS and ES should be noted. It makes it difficult to choose the right method for producing ferroelectric nonwoven materials, which meets the requirements of a particular application area.

The aim of our work was to investigate the production method influence (SBS and ES) on the structure and properties of the ferroelectric nonwoven materials based on VDF-TeFE copolymer.

VDF-TeFE copolymer was chosen for the nonwoven materials production because it has higher values of the strength and elongation [43], degree of crystallinity [44], pyroelectric coefficient [45] and electrostrictive constant [46] in comparison with PVDF.

2. Materials and methods

2.1. Nonwoven materials production

Previously it was shown that the concentration of a spinning solution has the most significant effect on the mean fiber diameter and as a result on the properties of the nonwoven materials produced by ES and SBS [47–49,26].

In order to investigate the influence of the production method on structure and properties of the nonwoven materials we have prepared five different spinning solutions with the following concentrations: 3, 5, 7, 9, and 11% (wt.). Statistical VDF-TeFE copolymer (Galopolymer, Russia) was utilized as a polymer material. To prepare the VDF-TeFE solutions a mixture of methylethylketone (Merck, Germany) and DMF (Sigma, USA) taken in a ratio of 1:2 (v/v) was used. PVDF-TeFE was dissolved in a sealed glass reactor at a temperature of 50 °C with constant stirring until a homogeneous transparent solution was obtained. The resulting solution was cooled to the room temperature.

The nonwoven materials were produced by ES using NANON-01A (MECC Co., Japan) equipment with the following technological parameters: a flow rate of the polymer solution of 10 ml/h, a distance from the needle to the collector of 16 cm, and a voltage of 20 kV.

Alternatively, the nonwoven materials were produced by SBS using equipment previously described in Refs. [50,51]. The following technological parameters were used: an air pressure of 0.4 MPa, a flow rate of the polymer solution of 50 ml/h, a nozzle diameter for supplying the polymeric solution of 0.6 mm, a nozzle diameter for supplying compressed air of 0.9 mm, and a distance from the nozzle to the collector of 30 cm.

2.2. Scanning electron microscopy (SEM)

The morphology of the nonwoven materials was investigated by scanning electron microscopy (SEM) JCM-6000 (JEOL, Japan). Prior to the investigation the material surface was coated with a thin layer of gold using magnetron-sputtering system SC7640 (Quorum Technologies Ltd, UK). The fiber diameter was determined from the SEM images out of 5 different fields of view using Image J 1.38 software (National Institutes of Health, USA). To calculate an average diameter at least 60 fibers were measured. The volume fraction was calculated with a method described by Sell et al. [52] as a ratio of the nonwoven materials density to the density of the film fabricated from the same polymer solution.

Please cite this article in press as: E.N. Bolbasov, et al., The investigation of the production method influence on the structure and properties of the ferroelectric nonwoven materials based on vinylidene fluoride − tetrafluoroethylene copolymer, Materials Chemistry and Physics (2016), http://dx.doi.org/10.1016/j.matchemphys.2016.07.041

2.3. Differential scanning calorimetry (DSC)

Differential scanning calorimetry (DSC) was used to determine the melting point (T_m), heat of fusion (ΔH_g), and change in the crystallinity degree ΔX_c (%). The studies were carried out on the differential scanning calorimeter DSC Q2000 (TA Instruments, USA) in a dry air atmosphere using a heating rate of 10 °C/min, and a temperature range of 80 °C–180 °C. The change in the crystallinity degree ΔX_c (%) of the nonwoven material compared with the raw powder of the copolymer VDF-TeFE was calculated from the following equation:

$$\Delta X_c = \left(\frac{H_{fs} - H_{fp}}{H_{fp}}\right) \times 100\% \quad (1)$$

where H_{fs} is the measured heat of fusion of the nonwoven material, and H_{fp} is the measured heat of fusion of the raw powder. It should be noted that the magnitude of H_f consists of the heat of fusion of both paraelectric and ferroelectric phases above the Curie temperature.

2.4. X-ray diffraction (XRD)

Investigation of the samples crystalline structure was conducted by X-ray diffraction analysis (Shimadzu XRD 6000, Japan). The average crystals size (l_c) was calculated using the Debye-Scherrer equation:

$$l_c = \frac{k\lambda}{\cos\theta\sqrt{\beta^2 - \beta_r^2}} \quad (2)$$

where λ is the wavelength of the incident radiation, β is the width of the reflection at a half height, β_r is the broadening reflex of the apparatus, θ is the angle of the diffraction and $k = 0.9$.

For DSC and XRD analysis the untreated VDF-TeFE copolymer powder was used as a control.

2.5. Mechanical strength

Tensile strength and relative elongation of the samples were investigated according to the recommendations of ISO 9073.3:1989 using Instron 3344 tensile testing machine (Instron, USA) with a sample preload of 0.1 N and a crosshead speed of 10 mm/min.

2.6. Cell studies

Cell adhesion was investigated by using two different cell types: multipotent mesenchymal stromal cells (MMSC) isolated from the mice bone marrow and endothelial hybrid cell line EA-hy 926. The materials were cut into a disk shape with a surface area of 1.8 cm^2 and placed in a 24-well plate. MMSC were cultured in a concentration of 2.5 × 10^5 cells/well in DMEM medium (Gibco, USA) containing a 1% HEPES buffer, 10% fetal bovine serum, 1% L-glutamine, 100 unit/ml penicillin, 0.1 mg/ml of streptomycin, and 0.1 μg/ml amphotericin B (Sigma Aldrich, USA). Cells from the endothelial hybrid cell line EA-hy 926 were cultured in a concentration of 2.5 × 10^5 cells/well in DMEM medium (Gibco, США) containing a 1% HEPES buffer, 10% fetal bovine serum, 1% L-glutamine, 100 unit/ml penicillin, 0.1 mg/ml of streptomycin, 0.1 μg/ml amphotericin B (Sigma Aldrich, USA), Aminopterin, and Thymidine (HAT) (Sigma Aldrich, USA). Cells cultured without materials were used as a control. Each material group (SBS, ES) including the control had 6 repeats. Cells were cultured for 5 days at 37 °C in 5% CO_2 atmosphere. The cell culture mediums were changed every 48 h.

In order to assess cell adhesion to the investigated materials, both cell types were stained with fluorescent dyes: PKH 26 (Sigma Aldrich, USA) for cell membranes and Hoechst 33342 (Sigma Aldrich, USA) for cell nucleus. The cell adhesion was evaluated by calculating the number of cells that are visible in ten fields of view of the fluorescent microscope Axio Observer Z1 (Carl Zeiss, Germany). Counted cell amount was then averaged and recalculated for 1 mm^2.

2.7. Statistical analysis

The statistical analysis was performed in Statistica (StatSoft, Dell) software using Mann–Whitney test. The differences between groups were considered significant at a significance level of $p < 0.05$.

3. Results and discussion

The SEM images of the nonwoven materials produced by ES and SBS from spinning solutions with different concentration are shown in Fig. 1.

The nonwoven material produced by ES from the spinning solution with a concentration of 3% were formed by the individual cylindrical-shaped fibers (Fig 1a) with the mean diameter of 0.38 ± 0.17 μm (Table 1). The spindle-shaped defects with the average size of 17 ± 4 μm on the longest axis could be found on the surface; the density of defects was 653 ± 78 pcs/mm^2. An increase in the VDF-TeFE copolymer concentration up to 5% led to an increase in the mean fiber diameter by more than 40% in comparison with the mean diameter of fibers formed from the spinning solution with a concentration of 3% (see Table 1). Meanwhile, a significant reduction in the defect density to 110 ± 24 pcs/mm^2 with a decrease in the average size of the defect to 12 ± 3 μm was observed (Fig 1c). An increase in the VDF-TeFE copolymer concentration up to 7% resulted in an increase of the mean fiber diameter up to 0.83 ± 0.53 μm. The individual defects were found on the material surface. The polydispersity of the fibers was increased (Fig. 1e) which is evidenced by an increase in the standard deviation of the mean fiber diameter (Table 1). When the nonwoven material was produced from the spinning solution with a concentration of 9% no defects were found on its surface. The formation of the own microrelief on the fibers surface was observed (Fig 1g) The polydispersity and the mean diameter of the fiber were increased (Table 1). At a spinning solution concentration of 11% the obtained nonwoven material contained a substantial amount of defects, moreover the fibers were glued together in the contact areas (Fig 1i).

In comparison with the material formed by ES, the nonwoven matrix produced by SBS from the spinning solution with a concentration of 3% had a multi-level spatial organization, where two types of elements could be distinguished (Fig 1b). The first type is macrostructures: fibers with a mean diameter of 8.3 ± 3.4 μm and globules with a mean diameter of 5.8 ± 2.2 μm. The density of the globules on the material surface was 3631 ± 435 pcs/mm^2. The space between the macrofibers was filled with the sub-micron microfibers of secondary structure with a mean diameter of 0.53 ± 0.16 μm (Table 1). These microfibers also formed the macrofibers mentioned above. The increase in the VDF-TeFE copolymer concentration up to 5% did not change the organization of the nonwoven material. The macrofibers remained in the material; moreover, their mean fiber diameter did not change significantly. However, the microfiber packing density in the macrofiber was decreased. The mean globules diameter was increased up to 9.8 ± 4.1 μm. At the same time, the globules density was decreased more than 3 times to 931 ± 125 pcs/mm^2. The polydispersity and

Please cite this article in press as: E.N. Bolbasov, et al., The investigation of the production method influence on the structure and properties of the ferroelectric nonwoven materials based on vinylidene fluoride – tetrafluoroethylene copolymer, Materials Chemistry and Physics (2016), http://dx.doi.org/10.1016/j.matchemphys.2016.07.041

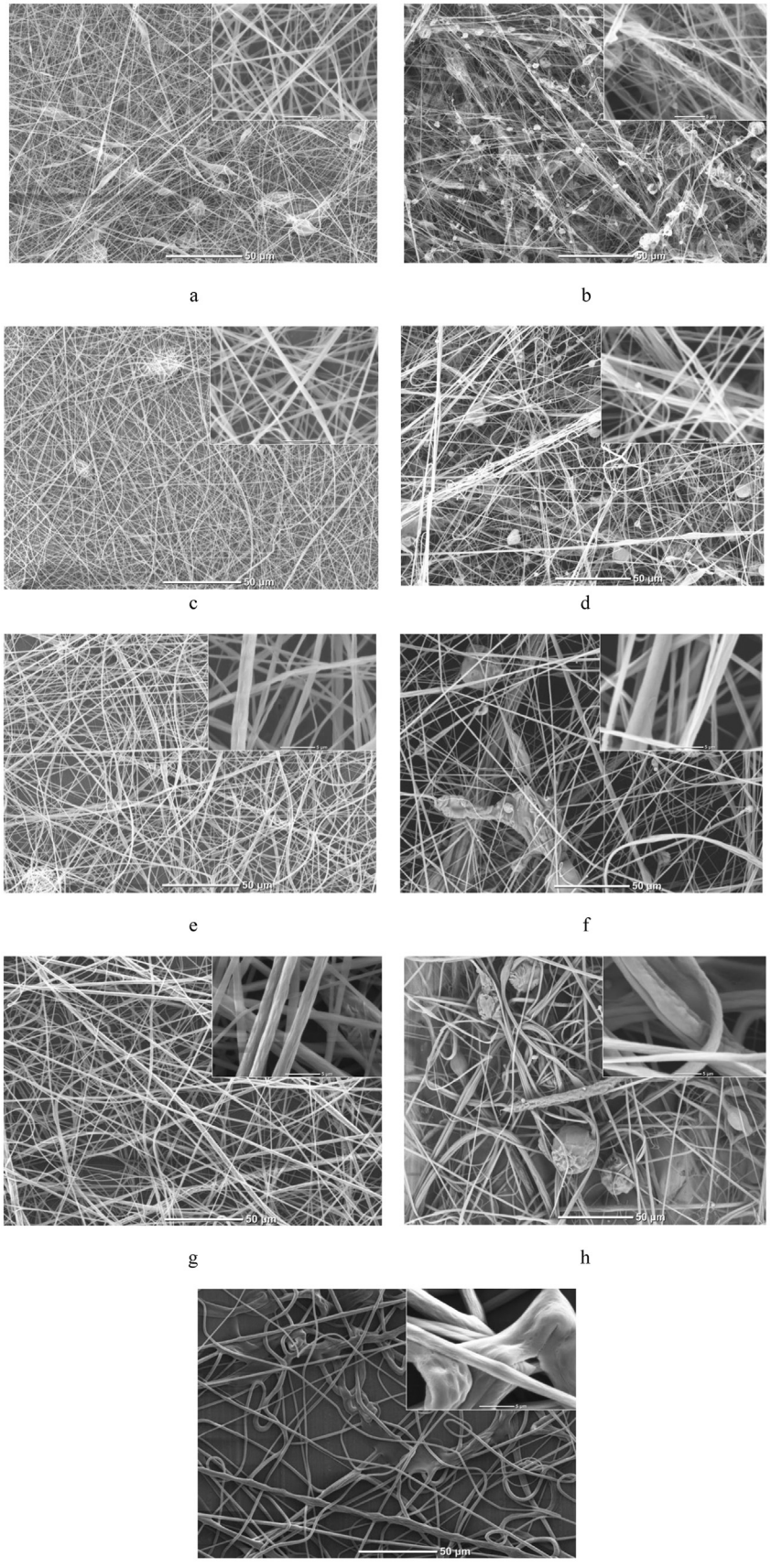

Fig. 1. The SEM images of the nonwoven materials obtained using spinning solutions with a different concentration of VDF-TeFE copolymer: a –ES 3% (wt.), c –ES 5% (wt.), e –ES 7% (wt.), g – ES 9% (wt.), i –ES 11% (wt.), b – SBS 3% (wt.), d – SBS 5% (wt.), f – SBS 7% (wt.), h – SBS 9% (wt.).

Please cite this article in press as: E.N. Bolbasov, et al., The investigation of the production method influence on the structure and properties of the ferroelectric nonwoven materials based on vinylidene fluoride – tetrafluoroethylene copolymer, Materials Chemistry and Physics (2016), http://dx.doi.org/10.1016/j.matchemphys.2016.07.041

Table 1
The dependency of the mean fiber diameter on the VDF-TeFE copolymer concentration in the spinning solution.

The VDF-TeFE copolymer concentration in the spinning solution, % (wt.)				
3	5	7	9	11
ES mean fiber diameter, μm				
0.38 ± 0.17	0.64 ± 0.29	0.83 ± 0.53	1.18 ± 0.67	1.71 ± 0.73
SBS mean fiber diameter, μm				
0.53 ± 0.16	0.77 ± 0.32	1.24 ± 0.58	2.81 ± 1.44	–

the mean diameter of the fiber were increased (Table 1). The formation of the own fiber microrelief on the microfiber surface was observed (Fig. 1 d). The increase of the VDF-TeFE copolymer concentration up to 7% led to the appearance of the large surface defects. Additionally, the fiber packing density was dramatically decreased. The polydispersity and the mean diameter of the fiber were increased (Table 1). The nonwoven materials produced by SBS from the spinning solution with a concentration of 9% had the largest amount of defects and were characterized by the low fiber packing density, the presence of a glued fibers and globules with the size of 30 μm. The nonwoven materials from the spinning solution with a VDF-TeFE concentration of 9% were not produced since the sprayer injection nozzle became clogged.

The analysis of the results shows that at the similar concentrations of the VDF-TeFE copolymer in the spinning solution the mean diameter of the fibers produced by ES is less than the mean diameter of fibers produced by SBS. This is consistent with the results obtained previously [35]. The ES is less sensitive to the polymer concentration in the spinning solution, which allows us to obtain the nonwoven materials in a wide range of the solution viscosities. At the same time, the nonwoven materials obtained by SBS differ by complex spatial organization. The similar fiber structure has been previously described when polymethylmethacrylate, polylactic acid and poly-ε-caprolactone were used for the production of the nonwoven materials by SBS [27,42,43].

Apparently, the differences in the structure of nonwoven materials are caused by the different mechanisms of the fibers formation. It is known that the process of production of nonwoven materials by ES is characterized by a high concentration of the like electric charges in the spinning solution. As a result of the electrical forces, a jet of the polymer solution becomes transversely unstable and flattened, and after the turn across the lines of the external electric field it splits along its axis into two approximately equal volume jets, each of which can be split again. This process is repeated several times and lasts until the capillary pressure on the surface of the branched jets does not compensate the pressure of the electrical forces or the jet does not turn into a solid fiber by the solvent evaporation [49,53]. Thus, jet multiple splitting processes driven by the electric forces helps to reduce the fiber diameter and provides a smooth and uniform fiber surface.

When nonwoven materials are produced by SBS, the polymer solution jet is accelerated and stretched by nonisothermal high-velocity gas stream. Under such conditions, the effective stretching of the polymer solution jet occurs at a short distance ($\approx 100 \div 150$ μm) from an injection nozzle. Stretching of the polymer jet causes a decrease in its diameter about 100 times compared to the diameter at the outlet of the injection nozzle. At the same time the rate of the polymer jet increases significantly and its velocity is about 23% of that of the surrounding air. The reduction of the polymer jet diameter is accompanied by the intensive solvent removal, resulting in an increased viscosity [54]. Then the polymer solution jet enters the gas flow area with high turbulence where it is bended and entangled. A larger viscosity of the spinning solution in the turbulent region prevents the effective jet stretching and splitting into branch jets. However, the likelihood of neighbour jets presence increases that leads to the formation of the fibers with a complex morphology and predominantly micron size [55].

The spectrum of physical and chemical properties of the nonwoven materials produced from the same spinning solutions is primarily determined by the size of fibers that form the material [56,57]. Thus, the investigation of the production method influence on the properties of the obtained nonwoven materials could be provided only if the mean diameter of the fibers that form the material is equal. According to the results of the morphology studies, we have chosen materials produced by ES and SBS from the spinning solution with a VDF-TeFE concentration of 5% (wt.). These materials do not differ significantly in the mean fiber diameter and have low polydispersity.

The DSC curves of the investigated materials are presented in Fig. 2. In the DSC curve of the VDF-TeFE powder there are two spaced endothermic peaks: one at 102.6 °C and the other one near 142 °C. The first peak is related to the energy required for the reorganization of the polymer material's crystalline structure in the transition from the ferroelectric to paraelectric state. An endothermic effect of this process was 1.2 ± 0.3 J/g. The second and more intensive peak corresponds to the melting of the VDF-TeFE copolymer [58,59]. In this case the endothermic effect was 19.4 ± 0.9 J/g.

In the DSC curve of SBS nonwoven materials an endothermic effect of 1.8 ± 0.2 J/g was also observed. It is caused by the Curie transition, however the transition temperature increased more than 13 °C in comparison with VDF-TeFE powder. Also there is a 1 °C shift for the melting point. The total amount of heat taken for the melting of the nonwoven material produced by SBS was 21.2 ± 0.7 J/g. The increase of the crystallinity degree of the nonwoven material produced by SBS in comparison with VDF-TeFE powder calculated according to the Equation (2) was over 14%.

In the DSC curve of ES nonwoven materials an endothermic effect which corresponds to the Curie transition was observed at 134 °C. It is overlapped with an endothermic effect related to material melting at 144 °C. The total heat of fusion for these two processes is 27.1 ± 1.3 J/g. Thus, the increase of the crystallinity degree of the nonwoven material produced by ES in comparison with VDF-TeFE powder was over 30%.

The shift and subsequent merger of the endothermic effects associated with the melting and Curie transition while increasing the heat of fusion was previously described [60]. This was shown in

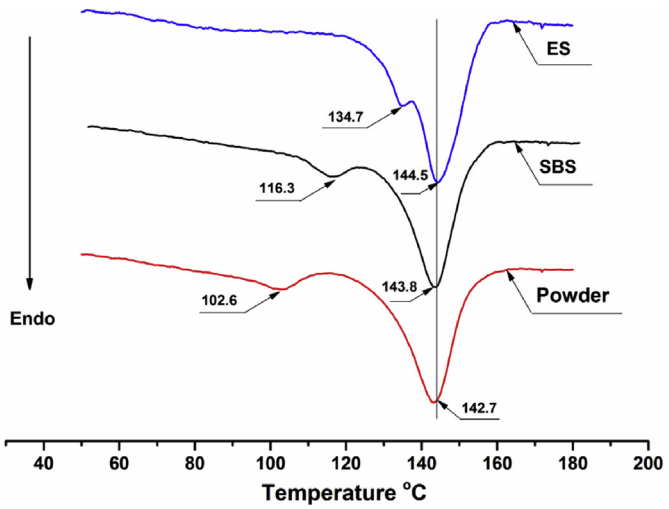

Fig. 2. The DSC curves of the investigated materials.

Please cite this article in press as: E.N. Bolbasov, et al., The investigation of the production method influence on the structure and properties of the ferroelectric nonwoven materials based on vinylidene fluoride – tetrafluoroethylene copolymer, Materials Chemistry and Physics (2016), http://dx.doi.org/10.1016/j.matchemphys.2016.07.041

VDF-TeFE copolymer samples with significant residual polarization after the exposure of polymer in electric fields of high intensity [60]. It is known that the effect of strong electric field and tensile forces on PVDF and its copolymers promote the ferroelectric phases formation [61]. Thus, the results of DSC allow us to suggest that both types of nonwoven materials have an increased amount of crystalline phases with ferroelectric properties. However, the influence of the electric field during the production of nonwoven materials by ES is more conducive than the formation of crystalline phases with ferroelectric properties.

The XRD patterns of the investigated materials are shown in Fig. 3.

The following reflexes could be found in the XRD patterns of the investigated materials: a halo in the 16–18° region corresponding to the paraelectric α – phase, a small diffraction peak in 18.6° area corresponding to the reflection from the plane (020) of the ferroelectric phase γ and an intensive diffraction peak in 19.3° region corresponding to the reflection from the planes (110, 200) of ferroelectric phase β [59]. In the VDF-TeFE powder XRD pattern there is a diffuse intramolecular reflex in the area of 35.5° corresponding to reflection from the (001) ferroelectric phase β. Also there is a peak in the area of 40.5° corresponding to the reflection from the (201, 111) of the ferroelectric phase β.

The nonwoven materials XRD patterns confirm rearrangement of the VDF-TeFE copolymer crystal structure under the tensile forces. These forces act on the spinning solution from the flow of the compressed gas or the electric field in the process of the materials production. It is proven by a decrease in the intensity of the halo in the area of 16–18°, which indicates a decrease in the ratio of the paraelectric α phase in the nonwoven materials in comparison with the VDF-TeFE powder. In the XRD pattern of the nonwoven material formed by SBS the intensity of reflexes in the area of 35° and 45° is significantly reduced with simultaneous increase of the intensity of the reflexes in the area of 19.2° (Table 2).

In the XRD pattern of the nonwoven material formed by the ES reflexes in the area of 35° and 45° were not found. There is almost no halo in the area of 16–18°. At the same time the intensity of the reflex of the ordered β phase in the direction of (110, 200) increases due to the extension and simultaneous polymer fibers polarization under the influence of a constant electric field arising in the space between the needle and the collector. It significantly increases the degree of crystallinity of the VDF-TeFE copolymer (Table 1). A significant increase in the degree of crystallinity after the production

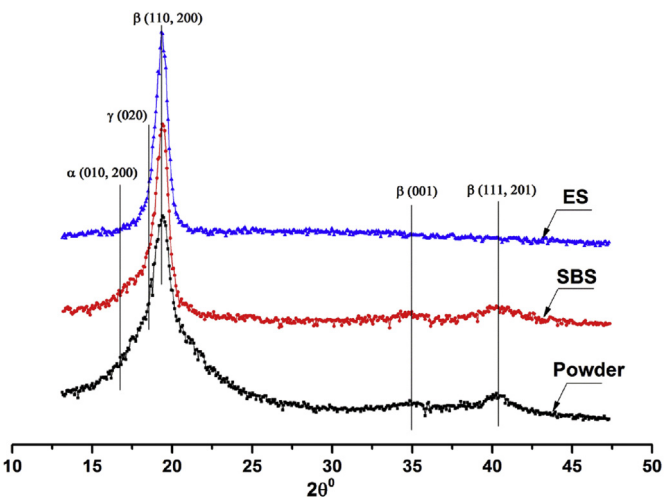

Fig. 3. The XRD patterns of the investigated materials.

Table 2
The crystallite size of the investigated materials.

Sample type	Powder	SBS	ES
Crystal size (nm) $\beta_{110,\ 200}$	5.4 ± 0.6	11.2 ± 0.3	14.4 ± 0.2

of PVDF and its copolymers-based nonwoven materials by ES was already described in several studies [26,62].

The results of nonwoven materials strength and relative elongation studies are shown in Table 3. It was found that the strength of the nonwoven materials formed by ES is more than 7.5 times higher than the strength of the nonwoven materials formed by SBS. An elongation at break is more than 1.3 times higher. Probably, these results may be caused by both the morphological and structural features of the obtained nonwoven material. The average volume fraction of the materials produced by ES was 21.3 ± 2.2%, which is approximately two times higher that the average volume fraction of the nonwoven materials produced by SBS – 12.3 ± 3.4%. Thus, the nonwoven materials produced by ES have lower porosity and, as a result, higher fiber packing density.

The high packing density of fibers in the nonwoven material produced by ES provides lower values of the specific load to each fiber, thus, increases strength. Additionally, the effect of the electric field promotes the formation of the β phase as it was shown by DSC and XRD. It is known that the production of nonwoven materials by ES stimulates an orientation of the ferroelectric β phase along the fiber axis. Thus, the β phase is well-ordered. The α phase has a much lower degree of orientation [63]. Since the amount of β phase in the nonwoven materials formed by ES is significantly higher in comparison with the nonwoven materials formed by the SBS, much more energy is required for the destruction of fibers. Therefore, the nonwoven materials formed by ES have significantly higher strength. The SEM images show that nonwoven materials produced by ES have a regular cylindrical shape. Nonwoven materials produced by SBS are characterized by an advanced microrelief. In addition, there are macrodefects in the form of droplets, and, at the same time, the density of defects is significantly higher. It is known that the defects occur in a crystalline solid reduce the mechanical strength of the latter. Thus, lower strength and elongation observed for nonwoven materials produced SBS are caused by structural defects.

The images of the fluorescently labelled cells are shown in Fig. 4.

The largest number of MMSC was observed in the control. The number of cells on the surface of the nonwoven materials produced by ES and SBS were reduced by 43% and 12% respectively in comparison with the control (Fig. 4). It could be explained by the high hydrophobicity of the PVDF and its copolymers, which prevents protein adsorption, and hence, cell adhesion. MMSC proliferated slowly and was not able to form a confluent monolayer within the culture period. Alternatively, the amount of EA-hy 926 cells was higher: 56% and 23% more for the nonwoven materials produced by ES and SBS respectively (Table 4) compared to the control. EA-hy 926 cell line has faster proliferation rate. In addition, tree-dimensional structure of the nonwoven materials allows cells to avoid the contact inhibition, thus, the amount of cells increased.

The differences in the amount of adhered cells between ES and SBS group may be caused by morphological and structural features

Table 3
Strength and relative elongation of the developed nonwoven materials.

Nonwoven material	Uniaxial tensile strength, kPa	Relative elongation, %
SBS	1920 ± 140	86 ± 14
ES	15300 ± 2600	122 ± 12

Please cite this article in press as: E.N. Bolbasov, et al., The investigation of the production method influence on the structure and properties of the ferroelectric nonwoven materials based on vinylidene fluoride – tetrafluoroethylene copolymer, Materials Chemistry and Physics (2016), http://dx.doi.org/10.1016/j.matchemphys.2016.07.041

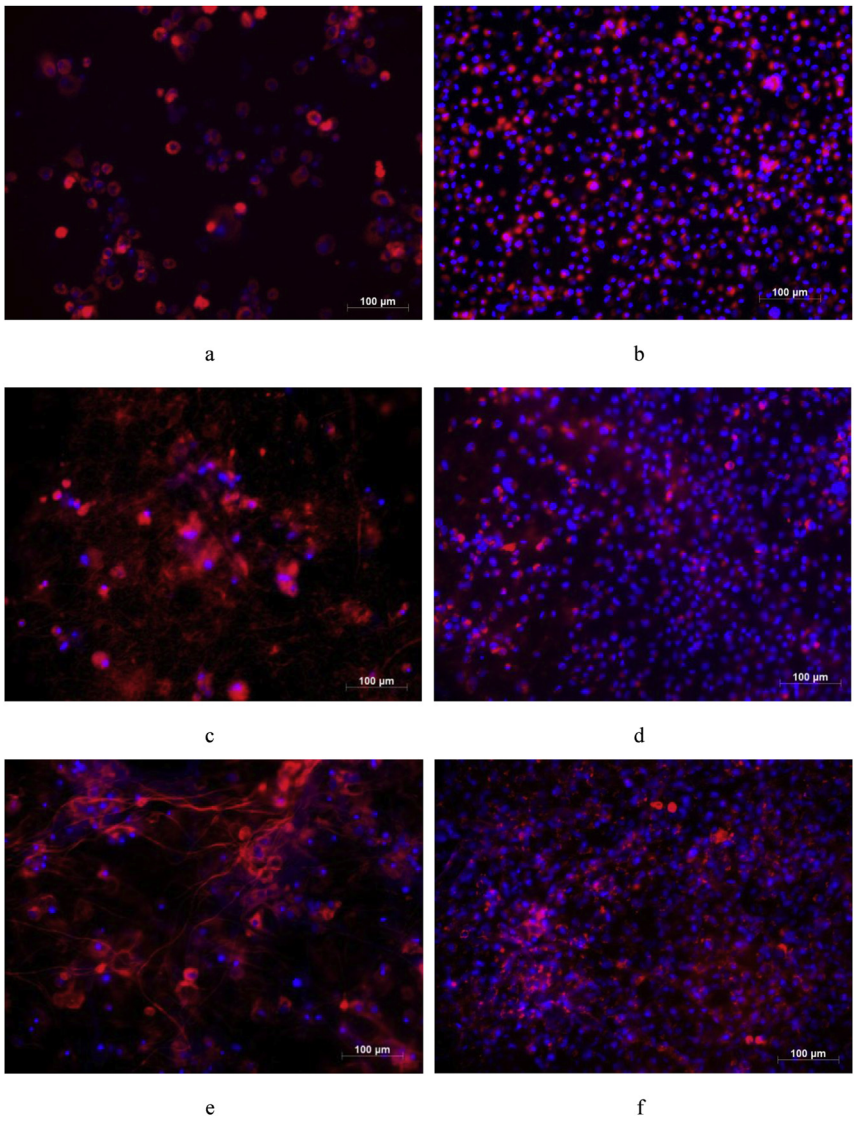

Fig. 4. The images of fluorescently labelled cells: a, c, and e – MMSC; b, d and f – EA-hy 926, (a, b) – control cell culture; (c, d) – cells on the surface of the nonwoven materials produced ES, (e, f) – cells on the surface of the nonwoven materials produced SBS. Cell membranes stained with PHK26 are visualized in red; cell nucleus stained with Hoechst 33342 are visualized in blue. (For interpretation of the references to colour in this figure legend, the reader is referred to the web version of this article.)

Table 4
The amount of MMSC and EA-hy 926 cells cultured on different nonwoven materials.

Sample type	Control	SBS	ES
MMSC			
Amount of cells per 1 mm^2, Me (25%; 75%).	446 (440; 506)	395[a,b] (358; 483)	195[a] (143; 340)
EA-hy 926			
Amount of cells per 1 mm^2, Me (25%; 75%)	2269 (1722; 2650)	3561[a,b] (3200; 3580)	2923[a] (2095; 3490)

[a] $p < 0,05$ (in comparison with control).
[b] $p < 0,05$ (in comparison with nonwoven materials produced by ES).

of the produced nonwoven materials.

It is known that cells adhere well to rough surfaces [64], thus an advanced surface of the fiber produced by SBS stimulates cell attachment. In addition, the large number of cells adhered on the surface of nonwoven materials produced by SBS was caused by the higher porosity and larger pore sizes observed in this type of material. These features also facilitate the migration of cells into a bulk of the nonwoven material and create the favourable conditions for the receipt of nutrients and removal of cells by-products [65]. A smaller number of cells that were found on the nonwoven materials obtained by ES is due to the high content of well-ordered ferroelectric β phase. In response to mechanical action it causes a significant change in surface potential values substantially exceeding the value needed to promote cell adhesion. The reduction of the number of adhered cells with an increase of ferroelectric β phase content was described previously [66]. Thus, the existence of an optimal quantity and quality of the ferroelectric β phase which will provide high levels of cell adhesion values can be assumed.

Please cite this article in press as: E.N. Bolbasov, et al., The investigation of the production method influence on the structure and properties of the ferroelectric nonwoven materials based on vinylidene fluoride – tetrafluoroethylene copolymer, Materials Chemistry and Physics (2016), http://dx.doi.org/10.1016/j.matchemphys.2016.07.041

4. Conclusions

The results of comparative studies of the structure and properties of the VDF-TeFE-based ferroelectric nonwoven materials obtained by ES and SBS were presented. It was shown that the nonwoven materials produced by ES have higher strength and relative elongation in comparison with the nonwoven materials produced by SBS. This is was caused by the differences in fibers morphology and crystalline structure. The nonwoven materials obtained by ES have high ferroelectric β − phase content and may be a good candidate for the following applications: sensors, energy generators, micro robots, etc. Moreover, such properties of nonwoven materials produced by SBS as the larger pore size, and rough fiber surface facilitates the penetration and adhesion of cells, which could potentially be used for tissue engineering.

Acknowledgments

This research was funded by Russian Science Foundation (project № 16-13-10239) and performed in Tomsk Polytechnic University: the comparative studies of structure and properties of nonwoven materials produced by electrospinning and solution blow spinning. The investigation of cell adhesion was performed in the Research Institute for Complex Issues of Cardiovascular Diseases under the funding of Russian Science Foundation (Project # 14-25-00050).

References

[1] B. Ameduri, From vinylidene fluoride (VDF) to the applications of VDF-containing polymers and copolymers: recent developments and future trends, Chem. Rev. 109 (2009) 6632–6686, http://dx.doi.org/10.1021/cr800187m.

[2] Z. Cui, E. Drioli, Y.M. Lee, Recent progress in fluoropolymers for membranes, Prog. Polym. Sci. 39 (2014) 164–198, http://dx.doi.org/10.1016/j.progpolymsci.2013.07.008.

[3] C. Feng, K.C. Khulbe, T. Matsuura, R. Gopal, S. Kaur, S. Ramakrishna, M. Khayet, Production of drinking water from saline water by air-gap membrane distillation using polyvinylidene fluoride nanofiber membrane, J. Memb. Sci. 311 (2008) 1–6, http://dx.doi.org/10.1016/j.memsci.2007.12.026.

[4] B.S. Lalia, E. Guillen-Burrieza, H.A. Arafat, R. Hashaikeh, Fabrication and characterization of polyvinylidenefluoride-co-hexafluoropropylene (PVDF-HFP) electrospun membranes for direct contact membrane distillation, J. Memb. Sci. 428 (2013) 104–115, http://dx.doi.org/10.1016/j.memsci.2012.10.061.

[5] K. Hwang, B. Kwon, H. Byun, Preparation of PVdF nanofiber membranes by electrospinning and their use as secondary battery separators, J. Memb. Sci. 378 (2011) 111–116, http://dx.doi.org/10.1016/j.memsci.2011.06.005.

[6] C.M. Costa, V. Sencadas, J.G. Rocha, M.M. Silva, S. Lanceros-Méndez, Evaluation of the main processing parameters influencing the performance of poly(-vinylidene fluoride-trifluoroethylene) lithium-ion battery separators, J. Solid State Electrochem. 17 (2013) 861–870, http://dx.doi.org/10.1007/s10008-012-1928-8.

[7] Y.-J. Kim, C.H. Ahn, M.B. Lee, M.-S. Choi, Characteristics of electrospun PVDF/SiO2 composite nanofiber membranes as polymer electrolyte, Mater. Chem. Phys. 127 (2011) 137–142, http://dx.doi.org/10.1016/j.matchemphys.2011.01.046.

[8] P. Martins, A.C. Lopes, S. Lanceros-Mendez, Electroactive phases of poly(-vinylidene fluoride): determination, processing and applications, Prog. Polym. Sci. 39 (2014) 683–706, http://dx.doi.org/10.1016/j.progpolymsci.2013.07.006.

[9] E. Cho, C. Kim, J.-K. Kook, Y. Il Jeong, J.H. Kim, Y.A. Kim, M. Endo, C.H. Hwang, Fabrication of electrospun PVDF nanofiber membrane for Western blot with high sensitivity, J. Memb. Sci. 389 (2012) 349–354, http://dx.doi.org/10.1016/j.memsci.2011.10.047.

[10] J. Chang, M. Dommer, C. Chang, L. Lin, Piezoelectric nanofibers for energy scavenging applications, Nano Energy 1 (2012) 356–371, http://dx.doi.org/10.1016/j.nanoen.2012.02.003.

[11] G. Ren, F. Cai, B. Li, J. Zheng, C. Xu, Flexible pressure sensor based on a poly(VDF-TrFE) nanofiber web, Macromol. Mater. Eng. 298 (2013) 541–546, http://dx.doi.org/10.1002/mame.201200218.

[12] L. Persano, C. Dagdeviren, Y. Su, Y. Zhang, S. Girardo, D. Pisignano, Y. Huang, J.A. Rogers, High performance piezoelectric devices based on aligned arrays of nanofibers of poly(vinylidenefluoride-co-trifluoroethylene), Nat. Commun. 4 (2013) 1633, http://dx.doi.org/10.1038/ncomms2639.

[13] F. He, B. Luo, S. Yuan, B. Liang, C. Choong, S.O. Pehkonen, PVDF film tethered with RGD-click-poly(glycidyl methacrylate) brushes by combination of direct surface-initiated ATRP and click chemistry for improved cytocompatibility, RSC Adv. 4 (2014) 105–117, http://dx.doi.org/10.1039/C3RA44789H.

[14] P. Hitscherich, S. Wu, R. Gordan, L.-H. Xie, T. Arinzeh, E.J. Lee, The effect of PVDF-TrFE scaffolds on stem cell derived cardiovascular cells, Biotechnol. Bioeng. 113 (2016) 1577–1585, http://dx.doi.org/10.1002/bit.25918.

[15] E.G. Fine, R.F. Valentini, R. Bellamkonda, P. Aebischer, Improved nerve regeneration through piezoelectric vinylidenefluoride-trifluoroethylene copolymer guidance channels, Biomaterials 12 (1991) 775–780, http://dx.doi.org/10.1016/0142-9612(91)90029-A.

[16] N. Royo-Gascon, M. Wininger, J.I. Scheinbeim, B.L. Firestein, W. Craelius, Piezoelectric substrates promote neurite growth in rat spinal cord neurons, Ann. Biomed. Eng. 41 (2013) 112–122, http://dx.doi.org/10.1007/s10439-012-0628-y.

[17] P. Lynen Jansen, U. Klinge, M. Anurov, S. Titkova, P.R. Mertens, M. Jansen, Surgical mesh as a scaffold for tissue regeneration in the esophagus, Eur. Surg. Res. 36 (2004) 104–111, http://dx.doi.org/10.1159/000076650.

[18] F.O. Agyemang, F.A. Sheikh, R. Appiah-Ntiamoah, J. Chandradass, H. Kim, Synthesis and characterization of poly (vinylidene fluoride)–calcium phosphate composite for potential tissue engineering applications, Ceram. Int. 41 (2015) 7066–7072, http://dx.doi.org/10.1016/j.ceramint.2015.02.014.

[19] J. Pärssinen, H. Hammarén, R. Rahikainen, V. Sencadas, C. Ribeiro, S. Vanhatupa, S. Miettinen, S. Lanceros-Méndez, V.P. Hytönen, Enhancement of adhesion and promotion of osteogenic differentiation of human adipose stem cells by poled electroactive poly(vinylidene fluoride), J. Biomed. Mater. Res. A (2014), http://dx.doi.org/10.1002/jbm.a.35234.

[20] A.M. Aronov, E.N. Bol'basov, V.V. Guzeev, M.V. Dvornichenko, S.I. Tverdokhlebov, I.A. Khlusov, Biological composites based on fluoropolymers with hydroxyapatite for intramedullary implants, Biomed. Eng. (NY) 44 (2010) 108–113, http://dx.doi.org/10.1007/s10527-010-9166-9.

[21] H.-F. Guo, Z.-S. Li, S.-W. Dong, W.-J. Chen, L. Deng, Y.-F. Wang, D.-J. Ying, Piezoelectric PU/PVDF electrospun scaffolds for wound healing applications, Colloids Surf. B Biointerfaces 96 (2012) 29–36, http://dx.doi.org/10.1016/j.colsurfb.2012.03.014.

[22] H. Salazar, A.C. Lima, A.C. Lopes, G. Botelho, S. Lanceros-Mendez, Poly(-vinylidene fluoride-trifluoroethylene)/NAY zeolite hybrid membranes as a drug release platform applied to ibuprofen release, Colloids Surf. A Physicochem. Eng. Asp. 469 (2015) 93–99, http://dx.doi.org/10.1016/j.colsurfa.2014.12.064.

[23] D. Gallego, N.J. Ferrell, D.J. Hansford, Fabrication of piezoelectric polyvinylidene fluoride (PVDF) microstructures by soft Lithography for tissue engineering and cell biology applications, MRS Proc. 1002 (2007), http://dx.doi.org/10.1557/PROC-1002-N04-05, 1002–N04–05.

[24] A.H. Rajabi, M. Jaffe, T.L. Arinzeh, Piezoelectric materials for tissue regeneration: a review, Acta Biomater. 24 (2015) 12–23, http://dx.doi.org/10.1016/j.actbio.2015.07.010.

[25] C. Ribeiro, V. Sencadas, D.M. Correia, S. Lanceros-Méndez, Piezoelectric polymers as biomaterials for tissue engineering applications, Colloids Surf. B Biointerfaces 136 (2015) 46–55, http://dx.doi.org/10.1016/j.colsurfb.2015.08.043.

[26] V. Sencadas, C. Ribeiro, J. Nunes-Pereira, V. Correia, S. Lanceros-Méndez, Fiber average size and distribution dependence on the electrospinning parameters of poly(vinylidene fluoride-trifluoroethylene) membranes for biomedical applications, Appl. Phys. A Mater. Sci. Process 109 (2012) 685–691, http://dx.doi.org/10.1007/s00339-012-7101-5.

[27] Y.-S. Lee, T.L. Arinzeh, The influence of piezoelectric scaffolds on neural differentiation of human neural stem/progenitor cells, Tissue Eng. Part A 18 (2012) 2063–2072, http://dx.doi.org/10.1089/ten.TEA.2011.0540.

[28] S.M. Damaraju, S. Wu, M. Jaffe, T.L. Arinzeh, Structural changes in PVDF fibers due to electrospinning and its effect on biological function, Biomed. Mater. 8 (2013) 045007, http://dx.doi.org/10.1088/1748-6041/8/4/045007.

[29] A. Frenot, I.S. Chronakis, Polymer nanofibers assembled by electrospinning, Curr. Opin. Colloid Interface Sci. 8 (2003) 64–75, http://dx.doi.org/10.1016/S1359-0294(03)00004-9.

[30] A.M. Behrens, B.J. Casey, M.J. Sikorski, K.L. Wu, W. Tutak, A.D. Sandler, P. Kofinas, In Situ deposition of PLGA nanofibers via solution blow spinning, ACS Macro Lett. 3 (2014) 249–254, http://dx.doi.org/10.1021/mz500049x.

[31] D.D. da Silva Parize, M.M. Foschini, J.E. de Oliveira, A.P. Klamczynski, G.M. Glenn, J.M. Marconcini, L.H.C. Mattoso, Solution blow spinning: parameters optimization and effects on the properties of nanofibers from poly(lactic acid)/dimethyl carbonate solutions, J. Mater. Sci. 51 (2016) 4627–4638, http://dx.doi.org/10.1007/s10853-016-9778-x.

[32] G. Sabbatier, P. Abadie, F. Dieval, B. Durand, G. Laroche, Evaluation of an air spinning process to produce tailored biosynthetic nanofibre scaffolds, Mater. Sci. Eng. C. Mater. Biol. Appl. 35 (2014) 347–353, http://dx.doi.org/10.1016/j.msec.2013.11.004.

[33] X. Zhuang, L. Shi, K. Jia, B. Cheng, W. Kang, Solution blown nanofibrous membrane for microfiltration, J. Memb. Sci. 429 (2013) 66–70, http://dx.doi.org/10.1016/j.memsci.2012.11.036.

[34] H. Lou, W. Li, C. Li, X. Wang, Systematic investigation on parameters of solution blown micro/nanofibers using response surface methodology based on box-Behnken design, J. Appl. Polym. Sci. 130 (2013) 1383–1391, http://dx.doi.org/10.1002/app.39317.

[35] J.E. Oliveira, L.H.C. Mattoso, W.J. Orts, E.S. Medeiros, Structural and morphological characterization of micro and nanofibers produced by electrospinning

Please cite this article in press as: E.N. Bolbasov, et al., The investigation of the production method influence on the structure and properties of the ferroelectric nonwoven materials based on vinylidene fluoride − tetrafluoroethylene copolymer, Materials Chemistry and Physics (2016), http://dx.doi.org/10.1016/j.matchemphys.2016.07.041

and solution blow spinning: a comparative study, Adv. Mater. Sci. Eng. (2013), http://dx.doi.org/10.1155/2013/409572.
[36] M.A. Souza, K.Y. Sakamoto, L.H.C. Mattoso, Release of the diclofenac sodium by nanofibers of poly(3-hydroxybutyrate-co-3-hydroxyvalerate) obtained from electrospinning and solution blow spinning, J. Nanomater. (2014) 1–8, http://dx.doi.org/10.1155/2014/129035.
[37] M. Wojasiński, M. Pilarek, T. Ciach, Comparative studies of electrospinning and solution blow spinning processes for the production of nanofibrous poly(L-Lactic acid) materials for biomedical engineering, Pol. J. Chem. Technol. 16 (2014), http://dx.doi.org/10.2478/pjct-2014-0028.
[38] W. Tutak, S. Sarkar, S. Lin-Gibson, T.M. Farooque, G. Jyotsnendu, D. Wang, J. Kohn, D. Bolikal, C.G. Simon, The support of bone marrow stromal cell differentiation by airbrushed nanofiber scaffolds, Biomaterials 34 (2013) 2389–2398, http://dx.doi.org/10.1016/j.biomaterials.2012.12.020.
[39] V.V. Kochervinskii, Specifics of structural transformations in poly(vinylidene fluoride)-based ferroelectric polymers in high electric fields, Polym. Sci. Ser. C 50 (2008) 93–121, http://dx.doi.org/10.1134/S1811238208010062.
[40] K. Wei, H.-K. Kim, N. Kimura, H. Suzuki, H. Satou, K.-H. Lee, Y.-H. Park, I.-S. Kim, Effects of organic solvent and solution temperature on electrospun polyvinylidene fluoride nanofibers, J. Nanosci. Nanotechnol. 13 (2013) 2708–2713, http://dx.doi.org/10.1166/jnn.2013.7417.
[41] R. Neppalli, S. Wanjale, M. Birajdar, V. Causin, The effect of clay and of electrospinning on the polymorphism, structure and morphology of poly(-vinylidene fluoride), Eur. Polym. J. 49 (2013) 90–99, http://dx.doi.org/10.1016/j.eurpolymj.2012.09.023.
[42] S.M. Damaraju, S. Wu, M. Jaffe, T.L. Arinzeh, Structural changes in PVDF fibers due to electrospinning and its effect on biological function, Biomed. Mater 8 (2013) 045007, http://dx.doi.org/10.1088/1748-6041/8/4/045007.
[43] C. Feng, B. Shi, G. Li, Y. Wu, Preparation and properties of microporous membrane from poly(vinylidene fluoride-co-tetrafluoroethylene) (F2.4) for membrane distillation, J. Memb. Sci. 237 (2004) 15–24, http://dx.doi.org/10.1016/j.memsci.2004.02.007.
[44] S.M. Nakhmanson, M.B. Nardelli, J. Bernholc, Collective polarization effects in β -polyvinylidene fluoride and its copolymers with tri- and tetrafluoroethylene, Phys. Rev. B 72 (2005) 115210, http://dx.doi.org/10.1103/PhysRevB.72.115210.
[45] A.I. Baise, H. Lee, B. Oh, R.E. Salomon, M.M. Labes, Enhancement of pyroelectricity in a vinylidene fluoride–tetrafluoroethylene copolymer, Cit. Appl. Phys. Lett. J. Appl. Phys. 26 (1975), http://dx.doi.org/10.1063/1.335280.
[46] S. Tasaka, S. Miyata, Effects of crystal structure on piezoelectric and ferroelectric properties of copoly(vinylidenefluoride-tetrafluoroethylene), J. Appl. Phys. 57 (1985) 906, http://dx.doi.org/10.1063/1.334691.
[47] L. Shi, X. Zhuang, X. Tao, B. Cheng, W. Kang, Solution blowing nylon 6 nanofiber mats for air filtration, Fibers Polym. 14 (2013) 1485–1490, http://dx.doi.org/10.1007/s12221-013-1485-5.
[48] J.E. Oliveira, E.A. Moraes, R.G.F. Costa, A.S. Afonso, L.H.C. Mattoso, W.J. Orts, E.S. Medeiros, Nano and submicrometric fibers of poly(D,L-lactide) obtained by solution blow spinning: process and solution variables, J. Appl. Polym. Sci. 122 (2011) 3396–3405, http://dx.doi.org/10.1002/app.34410.
[49] V.K.Y. Filatov, A. Budyka, Electrospinning of Micro- and Nanofibers: Fundamentals in Separation and Filtration Processes, Begell House, Inc., 2007.
[50] E.N. Bol'basov, I.N. Lapin, S.I. Tverdokhlebov, V.A. Svetlichnyi, Aerodynamic synthesis of biocompatible matrices and their Functionalization by nanoparticles obtained by the method of laser ablation, Russ. Phys. J. 57 (2014) 293–300, http://dx.doi.org/10.1007/s11182-014-0238-2.
[51] E.N. Bolbasov, Y.G. Anissimov, A.V. Pustovoytov, I.A. Khlusov, A.A. Zaitsev, K.V. Zaitsev, I.N. Lapin, S.I. Tverdokhlebov, Ferroelectric polymer scaffolds based on a copolymer of tetrafluoroethylene with vinylidene fluoride: fabrication and properties, Mater. Sci. Eng. C. Mater. Biol. Appl. 40 (2014) 32–41, http://dx.doi.org/10.1016/j.msec.2014.03.038.
[52] S. Sell, C. Barnes, D. Simpson, G. Bowlin, Scaffold permeability as a means to determine fiber diameter and pore size of electrospun fibrinogen, J. Biomed. Mater. Res. Part A 85 (2008) 115–126, http://dx.doi.org/10.1002/jbm.a.31556.
[53] D. Lukáš, A. Sarkar, L. Martinová, K. Vodsed'álková, D. Lubasová, J. Chaloupek, P. Pokorný, P. Mikeš, J. Chvojka, M. Komárek, Physical principles of electrospinning (Electrospinning as a nano-scale technology of the twenty-first century), Text. Prog. 41 (2009) 59–140, http://dx.doi.org/10.1080/00405160902904641.
[54] S. Sinha-Ray, S. Sinha-Ray, A.L. Yarin, B. Pourdeyhimi, Theoretical and experimental investigation of physical mechanisms responsible for polymer nanofiber formation in solution blowing, Polym. Guildf. 56 (2015) 452–463, http://dx.doi.org/10.1016/j.polymer.2014.11.019.
[55] S. Sinha-Ray, A.L. Yarin, B. Pourdeyhimi, Meltblowing: I-basic physical mechanisms and threadline model, J. Appl. Phys. 108 (2010), http://dx.doi.org/10.1063/1.3457891.
[56] N. Bhardwaj, S.C. Kundu, Electrospinning: a fascinating fiber fabrication technique, Biotechnol. Adv. 28 (2010) 325–347, http://dx.doi.org/10.1016/j.biotechadv.2010.01.004.
[57] A. Basu, Progress in air-jet spinning, Text. Prog. 29 (1999) 1–38, http://dx.doi.org/10.1080/00405169908688877.
[58] Y. Murata, Curie transition in poled and unpoled copolymer of vinylidene fluoride and tetrafluoroethylene, Polym. J. 19 (1987) 337–346, http://dx.doi.org/10.1295/polymj.19.337.
[59] A.J. Lovinger, G.E. Johnson, H.E. Bair, E.W. Anderson, Structural, dielectric, and thermal investigation of the Curie transition in a tetrafluoroethylene copolymer of vinylidene fluoride, J. Appl. Phys. 56 (1984) 2412, http://dx.doi.org/10.1063/1.334303.
[60] Y. Murata, N. Koizumi, Ferroelectric behavior in vinylidene fluoride-tetrafluoroethylene copolymers, Ferroelectrics 92 (1989) 47–54, http://dx.doi.org/10.1080/00150198908211305.
[61] T. Furukawa, Ferroelectric properties of vinylidene fluoride copolymers, Phase Transit. 18 (1989) 143–211, http://dx.doi.org/10.1080/01411598908206863.
[62] N. Weber, Y.S. Lee, S. Shanmugasundaram, M. Jaffe, T.L. Arinzeh, Characterization and in vitro cytocompatibility of piezoelectric electrospun scaffolds, Acta Biomater. 6 (2010) 3550–3556, http://dx.doi.org/10.1016/j.actbio.2010.03.035.
[63] W.A. Yee, M. Kotaki, Y. Liu, X. Lu, Morphology, polymorphism behavior and molecular orientation of electrospun poly(vinylidene fluoride) fibers, Polym. Guildf. 48 (2007) 512–521, http://dx.doi.org/10.1016/j.polymer.2006.11.036.
[64] A.B. Faia-Torres, M. Charnley, T. Goren, S. Guimond-Lischer, M. Rottmar, K. Maniura-Weber, N.D. Spencer, R.L. Reis, M. Textor, N.M. Neves, Osteogenic differentiation of human mesenchymal stem cells in the absence of osteogenic supplements: a surface-roughness gradient study, Acta Biomater. 28 (2015) 64–75, http://dx.doi.org/10.1016/j.actbio.2015.09.028.
[65] M.Á. Brennan, A. Renaud, A. Gamblin, C. D'Arros, S. Nedellec, V. Trichet, P. Layrolle, 3D cell culture and osteogenic differentiation of human bone marrow stromal cells plated onto jet-sprayed or electrospun micro-fiber scaffolds, Biomed. Mater. 10 (2015) 045019, http://dx.doi.org/10.1088/1748-6041/10/4/045019.
[66] S.M. Damaraju, S. Wu, M. Jaffe, T.L. Arinzeh, Structural changes in PVDF fibers due to electrospinning and its effect on biological function, Biomed. Mater. 8 (2013) 045007, http://dx.doi.org/10.1088/1748-6041/8/4/045007.

Please cite this article in press as: E.N. Bolbasov, et al., The investigation of the production method influence on the structure and properties of the ferroelectric nonwoven materials based on vinylidene fluoride – tetrafluoroethylene copolymer, Materials Chemistry and Physics (2016), http://dx.doi.org/10.1016/j.matchemphys.2016.07.041